

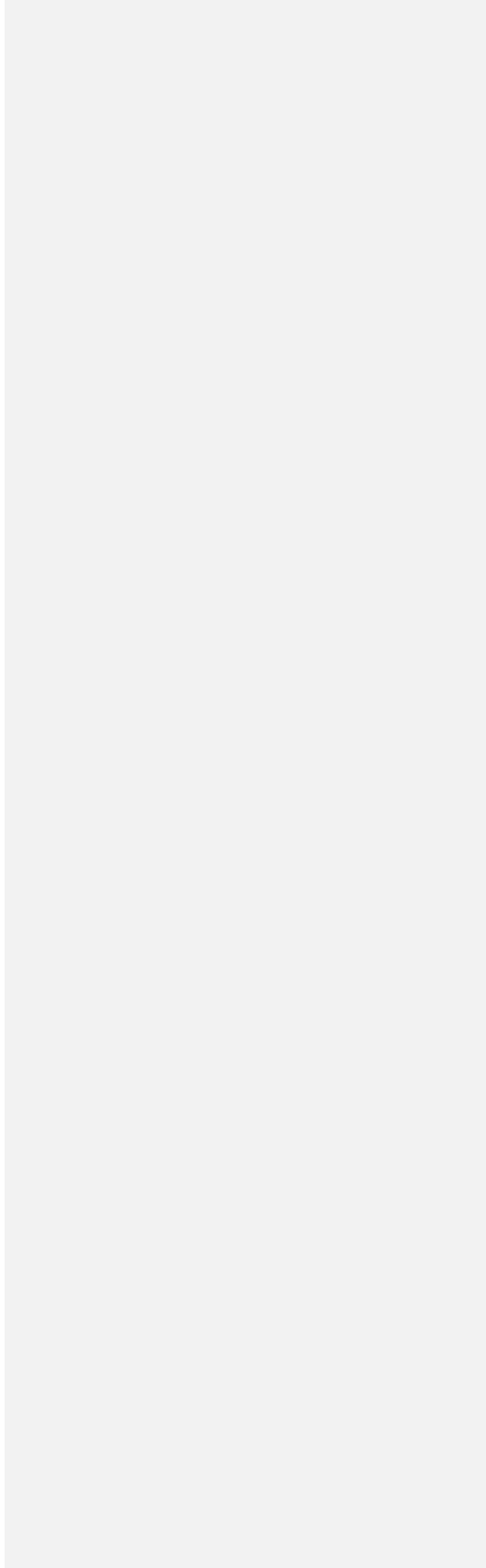
1
2
3
4
5
6
7
8
9
10
11
12
13
14
15
16
17
18
19
20
21
22
23
24
25
26
27
28
29
30
31
32
33
34

Technical Note:

A note on small-scale potential feedback mechanisms of large-scale ocean circulations
~~A note on stabilization mechanisms of, e.g., Atlantic Ocean meridional overturning circulation~~

by **Hans van Haren**

Royal Netherlands Institute for Sea Research (NIOZ), P.O. Box 59, 1790 AB Den Burg,
the Netherlands.
e-mail: hans.van.haren@nioz.nl



35 Short summary. The extent of mankind's influence on Earth's climate warrants ocean-studies.
36 A supposed major heat-transporter is the Atlantic Meridional Overturning Circulation
37 (AMOC). As AMOC is a complex nonlinear dynamical system, mathematical models may
38 predict its potential collapse using single parameters like surface temperature. However,
39 physical processes such as (sub-)mesoscale eddy transport and turbulent mixing by internal
40 wave breaking will alter the estimators, so that the AMOC may not collapse.

41

42 **Abstract.** The extent of anthropogenic influence on the Earth's climate warrants studies of
43 the ocean as a major player. Large, basin-wideThe ocean circulations areis important for
44 transporting properties like heat, carbon and nutrients. A supposed major conduit is the
45 Atlantic Meridional Overturning Circulation (AMOC). As the AMOC is a complex nonlinear
46 dynamical system, it is challenging to predict its potential to collapse and/or reversal of
47 direction from a statistical viewpoint using a single parameter like sea-surface temperature or
48 freshwater influx in numerical models. However, as is argued in this note supported by
49 spectra from ocean observations, small-scale physical processes such as, for example,
50 transport by sub-mesoscale eddies and turbulence-generating breaking of internal waves that
51 are not incorporated in these models will alter such parameters, and thereby statistical
52 analyses. This may lead to feed-back mechanisms on property gradients such as density
53 stratification so that large-scale ocean circulations like the AMOC may not collapse.

54

55 **1 Introduction**

56 Schematically, the Atlantic(-Ocean) Meridional Overturning Circulation (AMOC) is
57 depicted to transports heat from the equator to the poles near the surface and carbon in the
58 abyssal return (e.g., Aldama-Campino et al., 2023). It includes physical processes like 'deep
59 dense-water formation' in the polar region. Recent mathematical and numerical modelling
60 such as based on varying single parameters like sea-surface temperature (e.g., Ditlevsen and
61 Ditlevsen, 2023) and freshwater influx (e.g., van Westen et al., 2024) suggest a potential

62 future collapse of the AMOC. It is argued that this may have consequences for Northwest-
63 European climate.

64 Whilst the modelling might be robust mathematically, it lacks physical processes of
65 the drivers of the AMOC and observational evidence thereof. This will have consequences for
66 the feed-back mechanisms at work in the nonlinear dynamical system of ocean circulation. As
67 has been reviewed for AMOC numerical models (Gent, 2018), important feed-back
68 mechanisms are vertical (turbulent) mixing, (sub-)mesoscale gyre (eddy) transport, and the
69 coupling with the atmosphere. Here we elaborate on the importance of turbulence induced by
70 internal wave breaking, possibly coupling with sub-mesoscale eddies, and stability variations
71 in vertical density stratification for such feed-back, by reviewing insights from recent
72 modeling and deep-sea observations. In particular, the core of ocean motions is spectrally
73 investigated focusing on most energetic mesoscale, internal wave, and turbulence scales.

74 In contrast with the atmosphere, the ocean is not [an ineffective](#) heat engine (Wunsch
75 and Ferrari, 2004) [despite its heat transportation](#). As a result, the AMOC is not [predominantly](#)
76 buoyancy-driven via push by deep dense-water formation near the poles ([Marshall and Schott,](#)
77 [1999; Marotzke and Scott, 1999](#)), which notably occurs in sporadic pulses rather than
78 continuously. Instead, the AMOC is [mainly](#) wind- and tide-driven, with turbulent mixing by
79 internal wave breaking, [and possibly associated upwelling close to boundaries](#) ([Ferrari et al.,](#)
80 [2016](#)), being considered an important physics process of pull [that dominates over push by a](#)
81 [heat engine](#). Winds, near the ocean surface, and tides, via interaction with seafloor topography
82 deeper down, contribute about equally to generate internal waves that are found everywhere
83 in the ocean interior. Such waves break predominantly at ubiquitous underwater seamounts
84 and continental slopes.

85 Without turbulent mixing, the AMOC would be confined to a 100-m thick near-
86 surface layer and the deep-ocean would be a stagnant pool of cold water ([Munk and Wunsch,](#)
87 [1998 and Ferrari, 2004](#)). This is not the case however, and the solar heat is mixed from the
88 surface downward so that the ocean is stably stratified in density all the way into its deepest
89 trenches, as has been shown in hydrographic deep-ocean observations (Taira et al., 2005; van

90 Haren et al., 2021a). Although turbulent mixing by internal wave breaking in the ocean-
91 interior is insufficient by at least a factor of two to maintain the vertical density stratification
92 (e.g., Gregg, 1989, Polzin et al., 1997), such breaking along ocean boundaries has been
93 suggested to be more than sufficient (Munk, 1966; Polzin et al., 1997). Especially large
94 internal wave breaking is expected to occur above steeply sloping topography (Eriksen, 1982;
95 Thorpe, 1987; Sarkar and Scotti, 2017). Because there are more and larger seamounts than
96 mountains on land, equally abundant sloping seafloors lead to abundant turbulent mixing, as
97 has been charted from recent observations and modelling results summarized below.

98

99 **2 Recent internal wave breaking results**

100 Detailed observations and numerical modeling have revealed the extent of internal
101 tide breaking processes above ocean topography (van Haren and Gostiaux, 2012; Winters,
102 2015; Wynne-Cattanach et al., 2024). Quantification of the turbulent mixing shows that it
103 occurs with typical tidal-period-average values that are more than 100 times larger over (just)
104 super-critical slopes than open-ocean values. A super-critical seafloor slope is steeper than the
105 slope of internal wave characteristics. While ocean-wide tides energetically dominate internal
106 waves, not all seafloor slopes are super-critical for these waves. In contrast, nearly all seafloor
107 slopes are super-critical for (at least one component of) secondly energetic near-inertial
108 waves, which are generated via geostrophic adjustment following the passage or collapse of a
109 disturbance such as fronts or atmospheric storms on the rotating Earth. Under common
110 stratification, near-inertial waves are at the lowest frequency of freely propagating internal
111 waves. The highest frequency propagating internal waves, near the buoyancy frequency,
112 experience only vertical walls as super-critical seafloor slopes.

113 Within a tidal, or near-inertial, period, turbulence peaks in bursts of shorter duration
114 than half an hour when highly nonlinear internal waves propagate as internal bores up a
115 super-critical slope, once or twice a tidal cycle. The breaking of bores leads primarily to
116 convective, buoyancy-driven turbulence, rather than frictional shear-turbulence over the
117 sloping seafloor and occur at a wide variety of deep-sea and deep-ocean locations (e.g., van

118 Haren et al., 2013; van Haren et al., 2024). Between bores, the turbulent mixing varies by an
119 order of magnitude in intensity, with effects extending about 100 m vertically and several
120 kilometers horizontally from the seafloor. Although intermittently occurring at a given
121 position of the sloping seafloor and about 10% varying in arrival time, the turbulence is
122 generated internally by the tide, for about 60% (Wunsch and Ferrari, 2004), and by winds, for
123 about 40%, in a stratified ocean-environment. The turbulent bores also resuspend sediment
124 and thereby replenish nutrients away from the seafloor (Hosegood et al., 2004), important for
125 deep-sea life. Enhanced turbulent mixing above (sloping) boundaries has a demonstrated
126 effect on the outcome of general ocean circulation models (e.g., Scott and Marotzke, 2002),
127 with predicted subtle effects on upwelling near the seafloor (Ferrari et al., 2016).

128 The question is whether the intensity of internal-wave induced deep-ocean
129 turbulence is affected by variations in sea-surface temperature or salinity, with what
130 consequences for the AMOC. In considering these it should be noted that various properties
131 determine different equilibria. For example, deep dense-water formation does not only occur
132 in polar seas, but occasionally also in the at least 10°C warmer Mediterranean (Gascard,
133 1978), with an important contribution of atmospheric exchange due to orographic generated
134 winds affecting the preconditioning by cooling and drying of near-surface waters. Similarly,
135 internal waves occur in oceans and in the Mediterranean under stratification conditions that
136 vary over at least of magnitude in time and space, but tides are relatively weak in the
137 Mediterranean latter, and yet ‘sufficient’ turbulent diapycnal mixing, sufficient for
138 maintenance of deep-sea stratification and thereby driving overturning circulation, is
139 generated via (the breaking above topography of) near-inertial motions mainly (van Haren et
140 al., 2013). Further complications are expected from interactions of internal waves with (sub-
141 mesoscale eddies and potential consequences of varying intensity thereof, e.g., on seasonal
142 scales.

143

144 **3 Revisiting Mediterranean observations as an example proxy for ocean conditions**

145 In many physical oceanographic aspects of heat and salt budgets, large-scale water-
146 flow circulation, [strong boundary flow](#), eddies at sub-mesoscales, near-inertial motions
147 including gyroscopic waves and internal wave turbulence, the Mediterranean Sea can be
148 considered a sample for the state of the much larger oceans (e.g., Gascard, 1973; [Crepon et](#)
149 [al., 1982](#); Garrett, 1994; Millot, 1999; van Haren and Millot, 2004; Testor and Gascard,
150 2006). [Like in oceans, the Mediterranean seafloor reaches great depths and can be rugged](#)
151 [with steep slopes in places, including continental slopes incised by deep canyons](#).

152 In the Northwest Mediterranean, vertical density stratification varies markedly with
153 seasons and years, having relatively large near-surface values in summer and relatively low
154 values in winter. The proximity of extensive mountain ranges on land generates highly
155 variable winds that can cool and dry surface waters. In winter in weaker stratified waters, this
156 may lead to unstable conditions of buoyancy driven convection in an exchange of dense-water
157 sinking down, and less dense-waters up. Like in the polar regions, such exchange can be
158 observed daily in the upper 10 m from the sea-surface, regularly down to a few 100 m from
159 the surface, and seldom, once every 5-8 years (e.g., Rhein, 1995; Mertens and Schott, 1998),
160 down to the abyssal seafloor at about 2500 m. In contrast, horizontal density gradients
161 associate with forcing of a dynamically unstable boundary current and eddies at multiple 1-
162 100 km (sub-)mesoscales (e.g., [Crepon et al., 1982](#); Testor and Gascard, 2006). These eddy
163 motions may push relatively warm waters down, thereby increasing the weak stratification in
164 the deep-sea.

165 In summer, atmospheric disturbances are less intense, near-surface stratification is
166 large due to solar heating, and eddy activity associated with some continental boundary flows
167 is weaker (Albérola et al., 1995). This opens the possibility for detection of near-inertial wave
168 dominance in kinetic energy. In relatively strong stratification, mainly gravity-driven parts of
169 near-inertial waves generate largest vertical current differences ‘shear’ that destabilizes
170 stratification due to their relatively short vertical length-scale, not only in the Mediterranean
171 but also as observed in the Atlantic Ocean (van Haren, 2007). [This destabilization may lead to](#)
172 [small-10-m vertical scale layering of near-homogeneous waters throughout seas and oceans](#).

173 On larger-100-m vertical scales near-homogeneous waters occur in deep waters of the
174 Mediterranean as well as of North-Atlantic basins like the Bay of Biscay and Canary Basin.
175 In near-homogeneous water-layers with weak stratification, ~~the~~ gyroscopic, Earth-rotation-
176 driven, parts of near-inertial waves dominate and result in 0.1-1 km diameter sub-sub-
177 mesoscale tubes of slantwise rather than vertical convection (Emanuel, 1994; Marshall and
178 Schott, 1999; Straneo et al., 2002; van Haren and Millot, 2004). Hence, one may expect
179 frequency spectra of non-tidal dominated data from instruments moored in the Mediterranean
180 reveal convection and thus deep transport under winter and summer conditions.

181 It is noted that ocean-spectra may show peaks such as at narrowband tidal and at,
182 broader band, inertial frequencies, but they lack gaps. This lack of spectral gaps potentially
183 couples motions at sub-inertial with inertial-buoyancy internal wave with super-buoyancy
184 turbulence frequency ranges. However, it is unclear how such a coupling may work as some
185 motions represent two-dimensional (2D) eddies, some linear waves, some non-linear waves,
186 some anisotropic stratified turbulence, and some isotropic 3D turbulence. This is investigated
187 by re(newed) spectral analysis below, using, in analogy, slopes typical for investigating
188 energy cascades in turbulence research.

190 4 Uncommon slopes in revisited spectra

191 Kinetic energy (KE) spectra from historic moored current meter observations down to
192 mid-depth $z = -1100$ m in the Ligurian Sea under upper-sea strongly stratified ‘summer’ and
193 weakly stratified ‘winter’ conditions surely lack gaps (Fig. 1). Although these hourly sampled
194 data barely resolve the turbulence ranges at frequencies higher than the buoyancy frequency,
195 the internal wave continuum was suggested to scale with frequency ω like ω^p , with, on a log-
196 log plot, ‘spectral slope’ $p = -2.2 \pm 0.4$ (van Haren and Millot, 2003), independent of location
197 and season albeit with different KE (power) levels.

198 Within the uncertainty range, several possible explanations can be given for the
199 observed spectral slope. Internal gravity waves have been fitted to $p = -2 \pm 0.5$ but only for f

Formatted: Font: Bold

Formatted: Indent: First line: 0 cm

200 $\ll \omega \ll N$ (Garrett and Munk, 1972), where f denotes the inertial frequency involving Earth
201 rotation and N denotes the buoyancy frequency reflecting the square-root of vertical density
202 stratification. Considering that the data in Fig. 1 are from a site where locally $N = (3 \pm 2)f$,
203 irrespective of season (van Haren and Millot, 2003), alternative explanations were sought for
204 observed spectral slopes at sub-inertial frequencies $0.2 \text{ cpd} < \omega < f$. Cpd is short for ‘cycles
205 per day’. An obvious candidate is ‘fine-structure contamination’ of step functions passing
206 sensors which gives a theoretical value of $p = -2$ (Phillips, 1971; Reid, 1971). For their winter
207 data, van Haren and Millot (2003) attributed such a slope to evidence intense mesoscale
208 activity, because of the continuation of slope up to $\omega = 5 \text{ cpd}$ before rolling off to white noise
209 (slope 0). However, they did not elaborate. Below, the data in Fig. 1 are re-analyzed from [thea](#)
210 perspective of convection-turbulence.

211 Theoretical considerations of non-zero-mean flow convection-turbulence suggest a
212 spectral scaling in the buoyancy range having $p = -11/5 = -2.2$ for KE, and $p = -7/5$ for a(n
213 active) scalar quantity. This ‘BO’-scaling follows atmospheric and theoretical works by
214 Bolgiano (1959) and Obukhov (1959). The scaling was set-up for a stably stratified
215 (atmospheric) environment for the anisotropic part in which turbulent kinetic energy is
216 partially transferred to potential energy leading to turbulent convection. Later works extended
217 BO-scaling to purely buoyancy-driven turbulence, e.g., for Rayleigh-Bénard convection
218 (Lohse and Xia, 2010).

219 Laboratory experiments on such gravitationally driven convection are inconclusive on
220 BO-scaling. This scaling is confirmed for both KE and temperature in experiments by
221 Ashkenazi and Steinberg (1999), while only for scalars by Pawar and Arakeri (2016) who
222 found a slope of $p = -5/3$ for KE. The $p = -5/3$ -slope suggests dominance of shear-induced
223 turbulence of the inertial subrange for equilibrium (isotropic) turbulence cascade in the ‘KO’-
224 scaling (Kolmogorov, 1941; Obukhov, 1949), but should also be found in spectra of scalars
225 that are passive in this range. Obviously, scalars cannot be passive and active at the same time
226 and [in the same](#) space. This discrepancy between (types of) scaling between scalars and KE

227 may be because the laboratory experiments of Pawar and Arakeri (2016) were in zero mean
228 flow. Also, under sufficiently stable conditions without shear, no inertial subrange is expected
229 (Bolgiano, 1959). However, the spectral extent of BO-scaling is largely unknown albeit it is
230 more generally found adjacent to higher-frequency inertial subrange. While KO-scaling is
231 based on a forward cascade of energy, the direction of energy cascade is inconclusive for BO-
232 scaling and may be partially forward and partially backward, at least as reasoned for pure
233 buoyancy-driven convection-turbulence (Lohse and Xia, 2010). Probably, directions of
234 cascade change with locality in the flow, and perhaps depend on scale, which would also
235 imply that KO- and BO-scaling cannot be found at the same site.

236 Revisiting data from non-zero mean flow and (weakly) stratified deep-sea in Fig. 1
237 demonstrates the possibility of fit of $p = -11/5$ outside near-inertial harmonic peaks. In winter,
238 such a fit is observed consistently through the entire range of $0.2 < \omega < 5$ cpd. In traditional
239 terms, this frequency range covers the transition from mesoscale $\omega < f$, via internal wave $f <$
240 $\omega < N$, to turbulence $\omega > N$ motions. In summer, the $p = -11/5$ -slope is found at two different
241 KE levels for bands $0.2 < \omega < \omega_{\min}$ and $2\Omega < \omega < 5$ cpd at sub- and super-IGW frequencies,
242 respectively. Here, $\omega_{\min} < f$ denotes the minimum frequency bound for inertio-gravity waves
243 IGW (LeBlond and Mysak, 1978), and Ω the Earth rotational frequency. Maximum IGW
244 frequency is denoted by $\omega_{\max} > 2\Omega$. The plotted IGW-bounds $[\omega_{\min} \ \omega_{\max}]$ are for weakly
245 stratified, near-homogeneous layers in which $N = f$.

246 The bridge between the KE-levels at sub- and super-IGW is formed by the finitely
247 broad near-inertial peak. The base of this peak is proposed to slope like $p = -1$ reaching super-
248 IGW BO-scaling at about $\omega \approx 4$ cpd $\approx N$. Such $p = -1$ -slope has been observed for the KE-
249 spectral continuum between $[f \ N]$ from the deep Bay of Biscay, Northeast Atlantic Ocean
250 (van Haren et al., 2002). Theoretically, this slope represents spectral scaling of intermittency
251 of a weakly chaotic nonlinear system (Schuster, 1984), i.e., 3D dynamical systems that evolve
252 into self-organized critical structures of states which are minimally stable (Bak et al., 1987).
253 Such a spectral bridge, or hump, is expected for turbulence in unstable stratification, as has

254 been illustrated using atmospheric observations (Lin, 1969). It is attributed to the flow field
255 absorbing energy from the scalar temperature field as potential energy is transferred to kinetic
256 energy. It is not clear to what extent near-inertial internal waves contribute in a similar way to
257 spectral redistribution of energy in our oceanographic data.

258 These spectral observations suggest a dominance of convection cascade from sub-
259 meso- via IGW- to, probably because unresolved, turbulence-scales under high-energetic
260 winter-conditions as they show a continuous slope across their frequency ranges. Such a
261 cascade is also suggested observed under quieter summer conditions when, however, its is
262 masked by IGW that lead a cascade at $\omega > \omega_{\min}$. Especially the sub-inertial range of
263 apparent BO-scaling seems out of the turbulence range, unless waters are near-homogeneous
264 $N \rightarrow 0$ so that $\omega_{\min} \rightarrow 0$. This would extend not only IGW, notably gyroscopic waves, but
265 also turbulence, probably in the form of slantwise convection, to the (sub-)mesoscale range.

266 For the mesoscale range, the observations in Fig. 1 are supported by numerical
267 modeling results that have suggested eddy-KE has a broad range of spectral slopes between -3
268 $< p < -5/3$ (Storer et al., 2022), and by satellite altimetry observations that indicated, after
269 noise-correction and transfer to KE, a best-fit of $p = -2.28$ (Xu and Fu, 2012). No mention
270 was made of BO-scaling, but the correspondence seems evident.

271 As the KE in Fig. 1 is at least one order of magnitude larger in winter than in
272 summer, a near-inertial peak, if existent, will be part of the spectral continuum during the
273 former. Inspired by Western Mediterranean observations, Saint-Guilly (1972) proposed from
274 theoretical work that winter-time inertial KE is spread over a broad featureless band, like
275 quasi-gyroscopic waves that may be present between IGW-bounds $[\omega_{\min}, \omega_{\max}]$ for $N \sim f$
276 (LeBlond and Mysak, 1978; Gerkema et al., 2008). However, observations from the year-
277 round upper-layer-stratified central Western Mediterranean demonstrate that, also in deep
278 homogeneous $N = 0$ waters, a near-inertial peak is observed in KE-spectra (van Haren and
279 Millot, 2004). This may be attributed to a year-round source of atmospheric-generated inertial

280 waves that are the only internal waves that can propagate without reflection from well-
281 stratified to near-homogeneous layers and back (van Haren, 2023b).

282 Based on limited spectral observations, Gascard (1973) suggested the generation of
283 12-h stability waves (close to the buoyancy frequency of very weak stratification) that may
284 briefly force dense-water formation, thereby implicitly suggesting a link between internal
285 waves and (sub-)mesoscale eddies. As such eddies have estimated relative vorticity of $|\zeta| = f/2$
286 in the Western Mediterranean (Testor and Gascard, 2006), this addition to the planetary
287 vorticity (f) automatically widens the ‘effective’ near-inertial band $0.5f < f_{\text{eff}} < 1.5f$, which
288 bounds are close to IGW-bounds for $N = 0.8f$. One of the properties can be a modification of
289 near-inertial frequency (Perkins, 1976), and trapping with downward propagation of near-
290 inertial waves in anticyclonic eddies (Kunze, 1985; Voet et al., 2024). Such frequency
291 modification may add to local physics of inertial wave caustics due to latitudinal variation
292 (LeBlond and Mysak, 1978), which however can only lead up to 15% change in f in the
293 Mediterranean. Although found to be limited to the rather flat KE-spectral dip in the
294 immediate half-order-of-magnitude sub-inertial frequency band, standing vortical modes
295 (low-frequency non-propagating motions) of vertical length-scale < 10 m are suggested to be
296 as energetic as internal waves (Polzin et al., 2003). Alternatively, it has been suggested for
297 North-Atlantic observations that vortical modes may interact with internal waves, affecting
298 internal-wave shear that was peaking over $O(10)$ m vertical scales at IGW-frequencies in a
299 band with limits determined by weak stratification as in $N = f$ (van Haren, 2007).

300 For hypothetical $\omega_{\text{min}} = 0.2$ cpd, at which the observed spectral slope changes away
301 from $p = -11/5$ (Fig. 1), one would require $N = 0.21f$, which is almost unmeasurable and not
302 existent for any prolonged period even in the deep Northwestern Mediterranean, to the
303 knowledge of the author. However, it may reflect ω_{min} computed using $f_{\text{eff}} = 0.5f$ and $N = f_{\text{eff}}$,
304 noting that such conditions can only apply for part of the record. If so, it would reflect a direct
305 coupling between sub-mesoscale and IGW-motions with slantwise convection (Marshall and
306 Schott, 1999Straneo et al., 2002; van Haren and Millot, 2004; Gerkema et al., 2008). The $p =$

307 $-11/5$ is significantly distinguishable from -2 over a frequency range of nearly two orders of
308 magnitude, and from $-5/3$ over a range of just over half an order of magnitude (Fig. 1). The
309 roll-off to noise (slope 0), for $\omega > 5$ cpd, may partially be seen as following a slope of $p = -5/3$
310 before 0. The roll-off around 0.1 cpd suggests an unresolved broad mesoscale peak-value
311 between 0.01 and 0.1 cpd. While these 1980's moored current meter data barely resolved the
312 turbulence part of the KE-spectrum, and thus also not the $p=-5/3$ inertial subrange slope, their
313 temperature sensors were too poor to simultaneously verify any spectral scaling for scalars.

314 About 40 years later, high-resolution moored temperature sensor 'T-' data provided
315 opportunity to verify scalar spectral scaling of turbulence energetic motions in the area. These
316 T-data evidenced occasional warming of the deep Northwest Mediterranean seafloor (Fig.
317 2a), which, after comparison with data from higher-up appeared to be coming from above, or
318 slanted sideways, under relatively stratified conditions (van Haren, 2023a). The data were
319 collected during mid-fall, when near-surface waters above were well-sufficiently stratified and
320 no (cooler) dense-water convection was formed. Locally near the seafloor, ~~T~~the broad two-
321 day warming around day 308 is most stratified, whilst during other periods waters are only
322 weakly stratified, including the quasi-inertial variations between days 316 and 322. These
323 weakly stratified near-inertial, or near-buoyancy as $N \approx f$, temperature variations may
324 evidence slantwise quasi-gyroscopic near-inertial waves, which can have a large vertical
325 component (LeBlond and Mysak, 1978), as opposed to more common near-horizontal near-
326 inertial waves in strongly stratified waters that are barely noticeable in temperature records.

327 The 18-day average spectra of the 2-s sampled data poorly resolve sub-mesoscales,
328 but show a well-resolved slope of $p = -1.4 \pm 0.025$ between $0.5 < \omega < 6000$ cpd, across the
329 IGW band and well into the turbulence band (Fig. 2b). No transition to a $-5/3$ -slope is
330 observed before roll-off to noise, but this does not exclude an inertial subrange at higher
331 frequencies hidden under white noise. The observed $p = -7/5$ -slope is found significantly
332 different from $p = -2$ and $-5/3$ over the indicated frequency range of four orders of magnitude
333 and over the ~~turbulence~~ range between $100 < \omega < 10^4$ cpd thereby representing convection

334 turbulence. Over a frequency range of half an order of magnitude the slope-error is about
335 ± 0.1 . Albeit not greatly resolved, the range between $\omega_{\max} < \omega < 10$ cpd falls-off steeper
336 roughly at $p = -2$ and the range between $10 < \omega < 100$ cpd shows a reduced variance that may
337 partially be characterized by intermittency ($p = -1$; Schuster, 1984), but which is not yet
338 explained. Here, it is observed to bridge between $p = -2$ and super-IGW BO-scaling $p = -7/5$.
339 This would be further observation of a marginally ocean-state to the -1-scaling in KE-spectra
340 (present Fig. 1 and van Haren et al., 2002) and in the continuum of the band [f N] in open-
341 ocean T-spectra (van Haren and Gostiaux, 2009).

342 Whilst more extended work with longer data sets is to be done, the extended
343 continuous spectral slope from these high-resolution temperature observations suggests a
344 direct coupling between sub-mesoscale motions, IGW motions, comprising internal gravity
345 and gyroscopic waves, and convection turbulence. The temperature spectra ~~are~~-also show
346 consistency with the limited KE-spectra of Fig. 1 from roughly the same area, and both
347 indicate a dominance of non-isotropic, stratified-turbulence convection between sub-
348 mesoscales and largest turbulent overturning scales in extended BO-scaling suggesting cross-
349 spectral coupling. The discrepancy with KE-spectra in laboratory experiments of Pawar and
350 Arakeri (2016) may be due to difference of settings. In a non-zero mean flow turbulence
351 convection experiment near the gas-liquid critical point, BO-scaling was observed for both
352 KE and temperature (Ashkenazi and Steinberg, 1999). We recall that our deep-sea conditions
353 are non-zero mean flow, weak tides, very high bulk Reynolds numbers $O(10^5)$ given the large
354 scales, ~~and~~-varying non-zero vertical density stratification, and our example spectra did not
355 resolve KO-scaling.

356 The mesoscale-IGW-turbulence motions transport and locally mix warm waters with
357 cooler surroundings~~downward~~. This contrasts with the process of buoyancy-driven dense-
358 water formation that is thought to bring cooler waters downward during short periods of time,
359 but for which no evidence exists in this 18-day T-sensor data set.

360

361 **54 How robust is the system of ocean circulation and stratification?**

362 Any variation to the nonlinear system of ocean circulation may encounter several
363 complex feedback mechanisms, of which the effects are not yet fully understood for the
364 present-day ocean. Although stable density stratification hampers vertical exchange by
365 turbulent mixing, it does not block it. While stratification supports internal waves and their
366 destabilizing shear, turbulent mixing during particular phase of a wave may decrease or
367 destroy it locally in time and space. However, a subsequent internal wave-phase will restratify
368 the mixed patch, thereby maintaining its own support of stable stratification. Such a feed-back
369 system may be at work, for example when the ocean absorbs more heat.

370 Increased sea-surface temperature may lead to increased vertical density
371 stratification, which may lead to less turbulent exchange as vertical overturning is suppressed.
372 However, it will also lead to more internal waves through the extension of their spectral band
373 to higher frequencies, with the potential to increased interaction, non-linearity, and
374 turbulence-generating wave breaking. As particular internal waves can propagate deep into
375 the ocean interior away from their source, they can cause enhanced turbulent mixing
376 elsewhere (e.g., Alford, 2003).

377 Limited observations have thus far not provided evidence for an inverse
378 correspondence between changes in turbulent mixing and changes in temperature across the
379 near-surface photic zone along a longitudinal section of the Northeast Atlantic Ocean (van
380 Haren et al., 2021b). This lack of correspondence suggests a feedback mechanism at work
381 mediating potential physical environment changes so that global warming may not affect
382 vertical turbulent fluxes of heat, and thereby also of, e.g., carbon. One such feedback
383 mechanism may be (convection-)turbulence induced by internal waves and sub-mesoscale
384 eddies. Re(newed)-analysis of yearlong moored current meter data from the Irminger Sea
385 (North-Atlantic Ocean) demonstrate a significant $p = -11/5$ spectral slope at sub- and at super-
386 inertial frequencies (Fig. 3). As was outlined in van Haren (2007), the area showed an IGW-
387 band (for $N = f$) with dominant sub-inertial shear at small 8-m vertical scales despite the
388 dominant internal tidal KE. The correspondence with the Mediterranean data of Fig. 1 is

389 striking, including the one order of magnitude change in KE between sub- and super-IGW $p =$
390 $-11/5$ -slopes with similar $p = -1$ bridge albeit uncertain crossing level, and similar heights of
391 near-inertial peak despite the tidal peak in Fig. 3.

392 While few ocean observations have been presented of BO-scaling thus far in
393 comparison with KO-scaling, coupling has not been established between convection and
394 stratified small-scale turbulence with mesoscale motions. Likewise, complicating factors
395 are spectral interruption by internal waves. However, internal wave trapping by mesoscale
396 eddies has been well described (e.g., Kunze, 1985; Voet et al., 2024), and which thus provides
397 an obvious coupling between these motions. It is expected that such coupling may lead to
398 strong nonlinearity (of the internal waves) that leads to turbulent mixing produced by wave
399 breaking. Although such turbulent mixing is smaller than that induced by internal wave
400 breaking above sloping topography, such coupling may be an important factor in downward
401 transport of near-inertial energy that eventually breaks elsewhere, e.g., over topography.

402 As demonstrated using Mediterranean observations, not only convectively unstable
403 cooler and/or saltier waters potentially lead to downward motions from the surface. Also, sub-
404 mesoscale eddies and near-inertial waves can convectively-push stratified waters to the deep
405 sea. Such a downward push can be fast to transport materials from surface to 2500-m deep
406 seafloor in a day (van Haren et al., 2006), and which speed is of the same order of magnitude
407 as attributed to dense-water convection (Schott et al., 1996). It can also be more turbulent
408 compared to shear-induced motions in the stratified ocean-interior, whereby turbulence
409 reaches the seafloor according to few observations from the abyssal Pacific (van Haren, 2020)
410 and alpine freshwater Lake Garda (van Haren and Dijkstra, 2021). Further extended
411 observational evidence is urgently needed, preferably resolving much larger scales.

412 Although the anthropogenic influence on the Earth's climate is without doubt, the
413 impact on ~~the~~ ocean circulation is not fully known because we lack sufficient, notably
414 observational, information of the relevant processes that can thus not be properly modeled
415 yet. Therefore, we should be cautious in making predictions such as in (e.g., Ditlevsen and
416 Ditlevsen, 2023; van Westen et al., 2024) on future ocean circulation based on single

417 parameters like ocean-surface temperature or fresh-water flux that are uncertain proxies.
418 Because no observational (van Haren et al., 2021b), modeling (Little et al., 2020) or paleo-
419 proxy validation (Cisneros et al., 2019) physics evidence exists that sea-surface temperature is
420 a solid estimator of AMOC-strength variations, other properties like vertical density gradients
421 (stratification), and turbulence intensity may be considered.

422 Variability of the ocean in space and time is a key to its dynamics, but it is unclear
423 how robust such variations can be, e.g., whether shifting sites for deep dense-water formation
424 (Gou et al., 2024) may be part of the same system. Observational evidence verifying
425 numerical simulations' outcome, not only predictions but also present-day, of ocean-state is
426 needed. Observations are also required to evidence variability in relevant physics processes
427 for model-implementation. Besides eddies and coupling with atmosphere (e.g., Gent, 2018),
428 numerical models of complex nonlinear ocean circulation should contain internal-wave
429 turbulence with appropriate space and time dependency. [The importance of \(internal wave
430 breaking leading to\) boundary mixing \(above sloping topography\) in general ocean
431 circulation models has been acknowledged in various ways \(Scott and Marotzke, 2002;
432 Ferrari et al., 2016\).](#)

433 As for the ocean circulation in the horizontal plane near its surface with most impact on
434 mankind, wind will remain the main driver rather than the AMOC. As long as the Earth
435 rotation does not alter direction, wind will maintain its general course (Wunsch, 2004). The
436 atmosphere remains the key player in the global heat transport across mid-latitudes rather than
437 the ocean. Simultaneously, the importance of processes like stratification and turbulent
438 mixing ~~indueedis induced~~ by, e.g., internal wave breaking with or without sub-mesoscale
439 coupling cannot be underestimated for life near the ocean-surface as well as in the -deep,
440 because it will come to a halt without such processes.

441

442 *Data availability.* No new data were created or analyzed in this study: replot and re-analysis
443 of data presented in van Haren and Millot (2003), in van Haren (2007) and in van Haren
444 (2023a).

445

446 *Competing interests.* The author declares that he has no conflict of interest.

447

448 *Acknowledgments.* I thank L. Gerringa for commenting [on](#) a previous draft of the manuscript.

449

450 **References**

- 451 Albrera, C., Millot, C., and Font, J.: On the seasonal and mesoscale variabilities of the
452 Northern Current during the PRIMO-0 experiment in the western Mediterranean Sea.
453 *Oceanol. Acta*, 18, 163-192, 1995.
- 454 Aldama-Campino A., Fransner F., Ödalen, M., Groeskamp, S., Yool, A. Döös, K., and
455 Nycander, J.: Meridional ocean carbon transport, *Global Biogeochem. Cy.*, 34
456 e2029GB006336, 2023.
- 457 [Alford, M. H.: Redistribution of energy available for ocean mixing by long-range propagation](#)
458 [of internal waves, *Nature*, 423, 159-162, 2003.](#)
- 459 Ashkenazi, S., and Steinberg, V.: Spectra and statistics of velocity and temperature
460 fluctuations in turbulent convection, *Phys. Rev. Lett.*, 83, 4760-4763, 1999.
- 461 Bak, P., Tang, C., and Wiesenfeld, K.: Self-organized criticality: An explanation of the 1/f
462 noise, *Phys. Rev. Lett.*, 59, 381-384, 1987.
- 463 Bolgiano, R.: Turbulent spectra in a stably stratified atmosphere, *J. Geophys. Res.*, 64, 2226-
464 2229, 1959.
- 465 Cisneros, M., Cacho, I., Frigola, J., Sanchez-Vidal, A., Calafat, A., Pedrosa-Pàmies, R.,
466 Rumín-Caparrós, A., and Canals, M.: Deep-water formation variability in the north-
467 western Mediterranean Sea during the last 2500 yr: A proxy validation with present-day
468 data, *Glob. Planet. Chang.* 177, 56-68, 2019.
- 469 [Crepon, M., Wald, L., and Monget, J. M.: Low-frequency waves in the Ligurian Sea during](#)
470 [December 1977, *J. Geophys. Res.*, 87, 595-600, 1982.](#)
- 471 Ditlevsen, P., and Ditlevsen, S.: Warning of a forthcoming collapse of the Atlantic meridional
472 overturning circulation, *Nat. Comm.* 14, 4254, 2023.
- 473 [Emanuel, K., *Atmospheric Convection 580 pp.*, Oxford Univ. Press, New York, 1984.](#)
- 474 Eriksen, C. C.: Observations of internal wave reflection off sloping bottoms, *J. Geophys.*
475 *Res.*, 87, 525-538, 1982.

476 [Ferrari, R., Mashayek, A., McDougall, T. J., Nikurashin, M. and Campin, J.-M.: Turning](#)
477 [ocean mixing upside down, *J. Phys. Oceanogr.*, 46, 2229-2261, 2016.](#)

478 Garrett, C.: The Mediterranean Sea as a climate test basin, In: Malanotte-Rizzoli, P., and
479 Robinson, A. R. eds., *Ocean Processes in Climate Dynamics: Global and Mediterranean*
480 *Examples*, Kluwer Academic Publishes, 227-237, 1994.

481 Garrett, C., and Munk, W.: Space-time scales of internal waves, *Geophys. Fluid Dyn.*, 3, 225-
482 264, 1972.

483 Gascard, J.-C.: Vertical motions in a region of deep water formation, *Deep-Sea Res.*, 20,
484 1011-1027, 1973.

485 Gascard, J.-C.: Mediterranean deep water formation, baroclinic eddies and ocean eddies,
486 *Oceanol. Acta*, 1, 315-330, 1978.

487 Gent, P. R.: A commentary on the Atlantic meridional overturning circulation stability on
488 climate models, *Ocean Mod.*, 122, 57-66, 2018.

489 Gerkema, T., Zimmerman, J. T. F., Maas, L. R. M., and van Haren, H.: Geophysical and
490 astrophysical fluid dynamics beyond the traditional approximation, *Rev. Geophys.*, 46,
491 RG2004, doi:10.1029/2006RG000220, 2008.

492 Gou, R., Wang, Y., Xiao, K., and Wu, L.: A plausible emergence of new convection sites in
493 the Arctic Ocean in a warming climate, *Environ. Res. Lett.*, 19, 031001, 2024.

494 Gregg, M. C.: Scaling turbulent dissipation in the thermocline, *J. Geophys. Res.*, 94, 9686-
495 9698, 1989.

496 Hosegood, P., Bonnin, J., and van Haren, H.: Solibore-induced sediment resuspension in the
497 Faeroe-Shetland Channel, *Geophys. Res. Lett.*, 31, L09301, doi:10.1029/2004GL019544,
498 2004.

499 Kolmogorov, A. N.: The local structure of turbulence in incompressible viscous fluid for very
500 large Reynolds numbers, *Dokl. Akad. Nauk SSSR*, 30, 301-305, 1941.

501 Kunze, E.: Near-inertial wave propagation in geostrophic shear, *J. Phys. Oceanogr.*, 15, 544-
502 565, 1985.

503 LeBlond, P. H., and Mysak, L. A.: *Waves in the ocean*, Elsevier, New York, 602 pp., 1978.

504 [Lin, J.-T., Turbulence spectra in the buoyancy subrange of thermally stratified shear flows,](#)
505 [143 pp., PhD-thesis Colorado State University, Fort Collins, 1969.](#)

506 Little, C. M., Zhao, M., and Buckley, M. W.: Do surface temperature indices reflect
507 centennial-timescale trends in Atlantic Meridional Overturning Circulation strength?
508 *Geophys. Res. Lett.*, 47, e2020GL090888, 2020.

509 Lohse, D., and Xia, K.-Q.: Small-Scale properties of turbulent Rayleigh-Bénard convection,
510 *Annu. Rev. Fluid Mech.*, 42, 335-364, 2010.

511 [Marotzke, J., and Scott, J. R.: Convective mixing and the thermohaline circulation, *J. Phys.*](#)
512 [Oceanogr.](#), 29, 2962-2970, 1999.

513 [Marshall, J., and Schott, F.: Open-ocean convection: observations, theory, and models, *Rev.*](#)
514 [Geophys.](#), 37, 1-64, 1999.

515 Mertens, C., and Schott, F.: Interannual variability of deep-water formation in the
516 Northwestern Mediterranean, *J. Phys. Oceanogr.*, 28, 1410-1424, 1998.

517 Millot, C.: Circulation in the Western Mediterranean Sea, *J. Mar. Sys.*, 20, 423-442, 1999.

518 Munk, W.: Abyssal recipes, *Deep-Sea Res.*, 13, 707-730, 1966.

519 [Munk, W., and Wunsch, C.: Abyssal recipes II: Energetics of tidal and wind mixing, *Deep-*](#)
520 [Sea Res. I](#), 45, 1977-2010, 1998.

521 Obukhov, A. M.: Structure of the temperature field in a turbulent flow, *Izv. Akad. Nauk*
522 *SSSR, Ser. Geogr. Geofiz.*, 13, 58-69, 1949.

523 Obukhov, A. M.: Effect of buoyancy forces on the structure of temperature field in a turbulent
524 flow, *Dokl. Akad. Nauk SSSR*, 125, 1246-1248, 1959.

525 Pawar, S. S., and Arakeri, J. H.: Kinetic energy and scalar spectra in high Rayleigh number
526 axially homogeneous buoyancy driven turbulence, *Phys. Fluids*, 28, 065103, 2016.

527 Perkins, H.: Observed effect of an eddy on inertial oscillations, *Deep-Sea Res.*, 23, 1037-
528 1042, 1976.

529 Phillips, O. M.: On spectra measured in an undulating layered medium, *J. Phys. Oceanogr.*, 1,
530 1-6, 1971.

531 Polzin, K. L., Toole, J. M., Ledwell, J. R., and Schmitt, R. W.: Spatial variability of turbulent
532 mixing in the abyssal ocean, *Science*, 276, 93-96, 1997.

533 Polzin, K. L., Kunze, E., Toole, J. M., and Schmitt, R. W.: The partition of finescale energy
534 into internal waves and subinertial motions, *J. Phys. Oceanogr.*, 33, 234-248, 2003.

535 Reid, R. O.: A special case of Phillips' general theory of sampling statistics for a layered
536 medium, *J. Phys. Oceanogr.*, 1, 61-62, 1971.

537 Rhein, M.: Deep water formation in the western Mediterranean, *J. Geophys. Res.*, 100, 6943-
538 6959, 1995.

539 Saint-Guilly, B.: On the response of the ocean to impulse, *Tellus* 24, 344-349, 1972.

540 Sarkar, S., and Scotti, A.: From topographic internal gravity waves to turbulence, *Ann. Rev.*
541 *Fluid Mech.*, 49, 195-220, 2017.

542 Schott, F., Visbeck, M., Send, U, Fischer, J., and Desaubies, Y.: Observations of deep
543 convection in the Gulf of Lions, Northern Mediterranean, during the winter of 1991/92, *J.*
544 *Phys. Oceanogr.*, 26, 505-524, 1996.

545 Schuster, H. G., *Deterministic Chaos: An Introduction*, Physik-Verlag, Weinheim, 220 pp.,
546 1984.

547 [Scott, J. R., and Marotzke, J., 1998: The location of diapycnal mixing and the meridional](#)
548 [overturning circulation, *J. Phys. Oceanogr.*, 32, 3578-3595, 2002.](#)

549 Storer, B. A., Buzzicotti, M., Khatri, H., Griffies, S. M., and Aluie, H.: Global energy
550 spectrum of the general oceanic circulation, *Nat. Comm.*, 13, 5314, 2022.

551 ~~Straneo, F., Kawase, M., and Riser, S. C.: Idealized models of slantwise convection in a~~
552 ~~baroclinic flow, *J. Phys. Oceanogr.*, 32, 558-572, 2002.~~

553 Taira, K., Yanagimoto D., and Kitagawa, S.: Deep CTD casts in the challenger deep. Mariana
554 Trench, *J. Oceanogr.*, 61, 447-454, 2005.

555 Testor, P., and Gascard, J.C.: Post-convection spreading phase in the Northwestern
556 Mediterranean Sea, *Deep-Sea Res.*, 53, 869-893, 2006.

557 Thorpe, S. A.: Transitional phenomena and the development of turbulence in stratified fluids:
558 a review, *J. Geophys. Res.*, 92, 5231-5248, 1987.

559 van Haren, H.: Inertial and tidal shear variability above Reykjanes Ridge, *Deep-Sea. Res. I*,
560 54, 856-870, 2007.

561 van Haren, H.: Slow persistent mixing in the abyss, *Ocean Dyn.*, 70, 339-352, 2020.

562 van Haren, H.: Convection and intermittency noise in water temperature near a deep
563 Mediterranean seafloor, *Phys. Fluids*, 35, 026604, 2023a.

564 van Haren, H.: Near-inertial wave propagation between stratified and homogeneous layers, *J.*
565 *Oceanogr.*, 79, 367-377, 2023b.

566 van Haren, H., and Dijkstra, H. A.: Convection under internal waves in an alpine lake, *Env.*
567 *Fluid Mech.*, 21, 305-316, 2021.

568 van Haren, H., and Gostiaux, L.: High-resolution open-ocean temperature spectra, *J.*
569 *Geophys. Res.*, 114, C05005, doi:10.1029/2008JC004967, 2009.

570 van Haren, H., and Gostiaux, L.: Detailed internal wave mixing observed above a deep-ocean
571 slope, *J. Mar. Res.*, 70, 173-197, 2012.

572 van Haren, H. and Millot, C.: Seasonality of internal gravity waves kinetic energy spectra in
573 the Ligurian Basin, *Oceanol. Acta*, 26, 635-644, 2003.

574 van Haren, H., and Millot, C.: Rectilinear and circular inertial motions in the Western
575 Mediterranean Sea, *Deep-Sea Res. I*, 51, 1441-1455, 2004.

576 van Haren, H., Maas, L., and van Aken, H.: On the nature of internal wave spectra near a
577 continental slope, *Geophys. Res. Lett.*, 29(12), 10.1029/2001GL014341, 2002.

578 van Haren, H., Millot, C., and Taupier-Letage, I.: Fast deep sinking in Mediterranean eddies,
579 *Geophys. Res. Lett.*, 33, L04606, doi:10.1029/2005GL025367, 2006.

580 van Haren, H., Ribó, M., and Puig, P.: (Sub-)inertial wave boundary turbulence in the Gulf of
581 Valencia. *J. Geophys. Res.Oceans*, 118, 2067-2073, doi:10.1002/jgrc.20168, 2013.

582 van Haren, H., Uchida, H., and Yanagimoto, D.: Further correcting pressure effects on
583 SBE911 CTD-conductivity data from hadal depths, *J. Oceanogr.*, 77, 137-144, 2021a.

584 van Haren, H., Brussaard, C. P. D., Gerringa, L. J. A., van Manen, M. H., Middag, R., and
585 Groenewegen, R.: Diapycnal mixing near the photic zone of the NE-Atlantic, *Ocean Sci.*,
586 17, 301-318, 2021b.

587 van Haren, H., Voet, G., Alford, M. H., Fernandez-Castro, B., Naveira Garabato, A. C.,
588 Wynne-Cattanach, B. L., Mercier, H., and Messias, M.-J.: Near-slope turbulence in a
589 Rockall canyon, *Deep-Sea Res. I*, 206, 104277, 2024.

590 van Westen, R. M., Kliphuis, M., and Dijkstra, H.A.: Physics-based early warning signal
591 shows that AMOC is on tipping course, *Sci. Adv.*, 10, eadk1189, 2024.

592 [Voet, G., et al.: Near-inertial energy variability in a strong mesoscale eddy field in the Iceland](#)
593 [Basin, *Oceanogr.*, 37, <https://doi.org/10.5670/oceanog.2024.302>, 2024.](#)

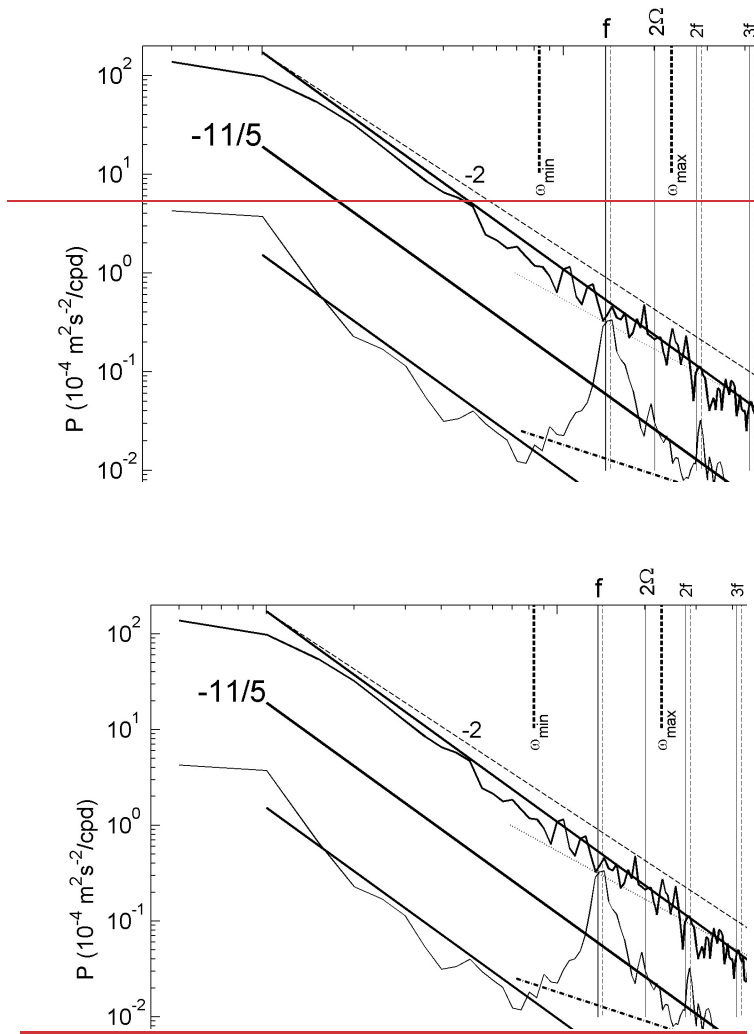
594 Winters, K. B.: Tidally driven mixing and dissipation in the stratified boundary layer above
595 steep submarine topography, *Geophys. Res. Lett.*, 42, 7123-7130, 2015.

596 Wunsch, C.: Gulf Stream safe if wind blows and Earth turns, *Nature*, 428, 601, 2004.

597 Wunsch, C., and Ferrari, R.: Vertical mixing, energy and the general circulation of the oceans,
598 *Ann. Rev. Fluid Mech.*, 36, 281-314, 2004.

599 Wynne-Cattanach, B. L., Couto, N., Drake, H. F., Ferrari, R., Le Boyer, A., Mercier, H.,
600 Messias, M.-J., Ruan, X., Spingys, C. P., van Haren, H., Voet, G., Polzin, K., Naveira
601 Garabato, A., and Alford, M. H.: Observational evidence of diapycnal upwelling within a
602 sloping submarine canyon, *Nature*, 630, 884-890, 2024.

603 Xu, Y., and Fu, L.-L.: The effects of altimeter instrument noise on the estimation of the
604 wavenumber spectrum of sea surface height, *J. Phys. Oceanogr.*, 42, 2229-2233, 2012.

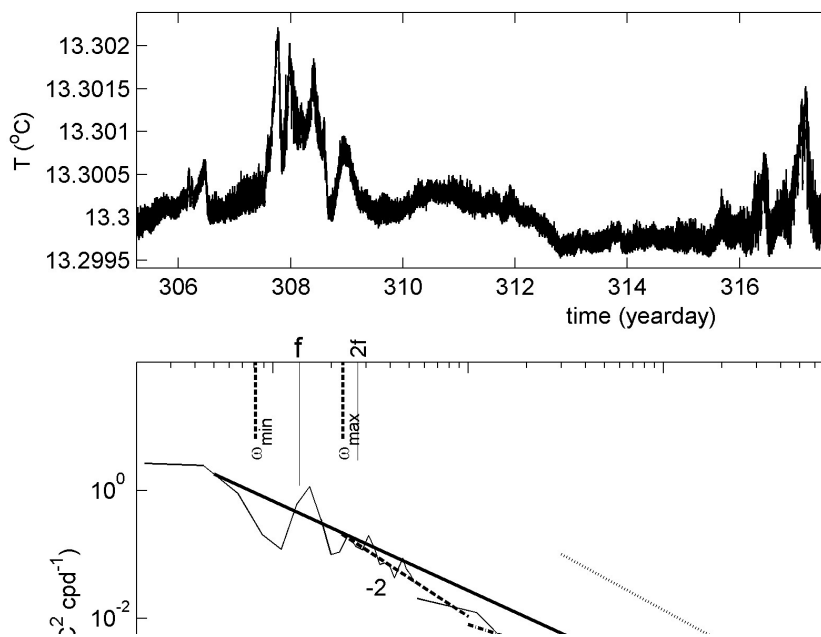


605

606

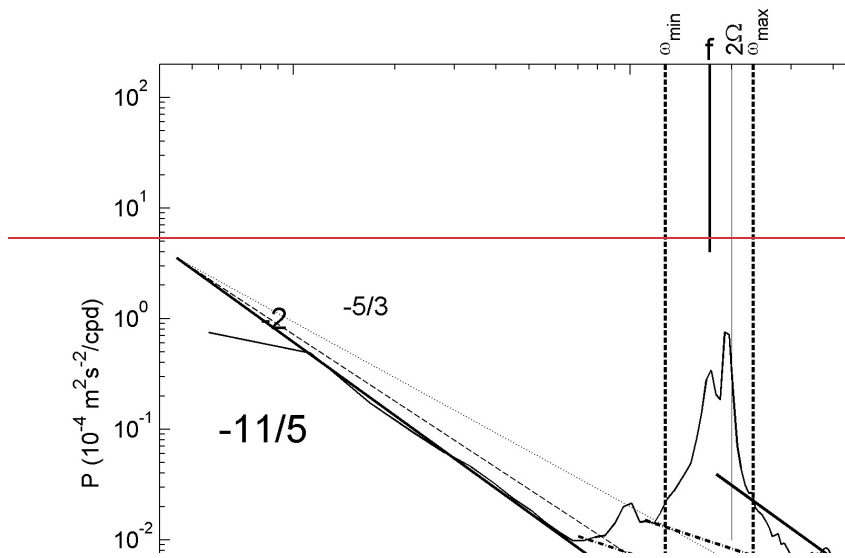
607 **Fig. 1.** Moderately smoothed (20 degrees of freedom, dof) kinetic energy (KE) spectra over
 608 100 days of data from 600-s sampled Aanderaa mechanical current meter moored in
 609 1981/1982 at $z = -1100$ m over the continental slope in the Ligurian Sea at $43^\circ 28.32' N$, 7°
 610 $46.10' E$, 2250 m water depth. For details on these data, see van Haren and Millot (2003). The
 611 ‘summer’ spectrum is an average from data between days 190 and 290 (in 1981), the ‘winter’

612 between days 375 and 475 (adding +365 for days in 1982). Several frequencies are indicated
 613 including inertial frequency f , Earth rotational Ω and inertio-gravity wave bounds [$\omega_{\min} < f$,
 614 $\omega_{\max} > N$] for buoyancy frequency $N = f$. The dashed lines indicate (harmonics of) $1.04f$. Four
 615 spectral slopes ω^p are indicated by their exponent: $p = -11/5$ (solid slope in the log-log plot)
 616 for Bolgiano-Obukhov ‘BO’ scaling reflecting the buoyancy subrange of convective
 617 turbulence (e.g., Pawar and Arakeri, 2016), $p = -5/3$ (dotted slope) for Kolmogorov-Obukhov
 618 ‘KO’ scaling reflecting the equilibrium inertial subrange for dominant shear-induced
 619 turbulence (Kolmogorov 1941; Obukhov, 1949), $p = -1$ (dash-dotted slope) for intermittency
 620 of self-organized criticality (Schuster, 1984; Bak et al., 1987) and $p = -2$ (dashed slope) for
 621 internal wave scaling (Garrett and Munk, 1972) or finestructure contamination (Phillips,
 622 1971; Reid, 1971).

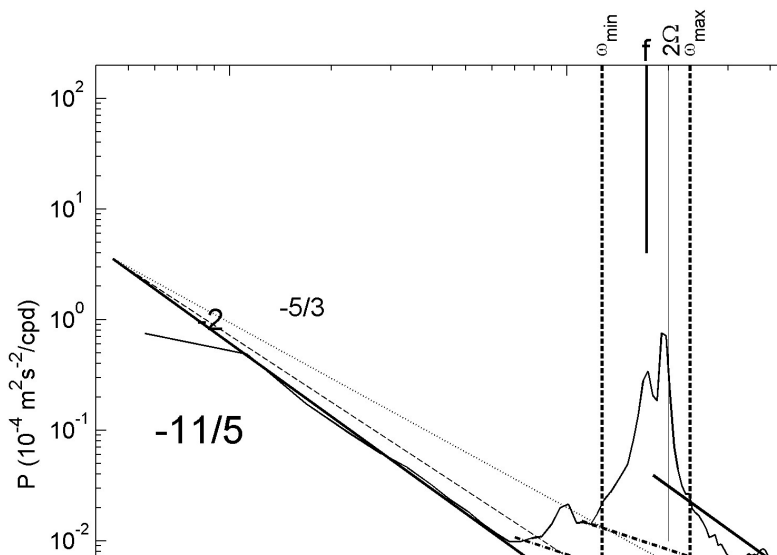


623
 624 **Fig. 2.** Eighteen days of high-resolution 2-s sampled temperature (T) data from a NIOZ
 625 T-sensor fallen off a mooring-line in 2020, and lying 0.01 m above a flat seafloor about
 626 10 km south of the foot of the continental slope at $42^\circ 49.50' N$, $6^\circ 11.78' E$, 2458 m
 627 water depth, about 100 km WSW from the site in Fig. 1. For details on these data see van

628 Haren (2023a). (a) Time series of 18 days of raw temperature data. (b) Weakly smoothed
629 (10 dof; $\omega < 5$ cpd) and heavily smoothed (250 dof; $\omega > 5$ cpd) temperature variance spectra
630 of data in a. Frequency and spectral slope indications as in Fig. 1, while $-7/5$ (solid slope)
631 indicates BO-scaling of an active scalar (e.g. Pawar and Arakeri, 2016), and -1 (dash-
632 dotted slope) for scaling of intermittency of a weakly chaotic nonlinear system (Schuster,
633 1984). Note the different axes-ranges compared with Fig. 1.



634



635

636

Fig. 3. Like Fig. 1, but for strongly smoothed (50 dof) KE spectra averaged over 400 days

637

of data from 600-s sampled Valeport mechanical current meter moored at $z = -1000$ m

638 over the Mid-Atlantic Ridge at 58° 59.67' N, 33° 56.12' W, 2540 m water depth in
639 2003/2004, within the project discussed in van Haren (2007).
640